ORIGINAL ARTICLE

Protective role of growth hormone against hyperhomocysteinemia-induced glomerular injury

**Caixia Li · Min Xia · Justine M. Abais · Xiaocheng Liu ·
Ningjun Li · Krishna M. Boini · Pin-Lan Li**

Abstract The present study investigated the protective role of growth hormone (GH) against hyperhomocysteinemia (hHcys)-induced activations of reactive oxygen species/hypoxia-inducible factor (HIF)-1α, epithelial–mesenchymal transition (EMT), and consequent glomerular injury. A hHcys model was induced by folate free diet in mice. The urine protein excretion significantly increased while plasma GH levels dramatically decreased in hHcys. Real-time reverse transcription polymerase chain reaction showed that GH receptor (GHR) level increased in the cortex of hHcys mice, which mainly occurred in podocytes as shown by confocal microscopy. Recombinant mouse growth hormone (rmGH) treatment (0.02 mg/kg, once a day for 6 weeks) significantly restored the plasma GH, inhibited GHR upregulation and attenuated proteinuria. Correspondingly, rmGH treatment also blocked hHcys-induced decrease in the expression of podocin, a podocyte slit diaphragm molecule, and inhibited the increases in the expression of desmin, a podocyte injury marker. It was also demonstrated that in hHcys the expression of epithelial markers, p-cadherin and ZO-1, decreased, while the expression of mesenchymal markers, antifibroblast-specific protein 1 (FSP-1) and α-SMA, increased in podocytes, which together suggest the activation of EMT in podocytes. Nicotinamide adenine dinucleotide phosphate oxidase (Nox)-dependent superoxide anion ($O_2^{\cdot-}$) and hypoxia-inducible factor-1α (HIF-1α) level in the hHcys mice cortex was markedly enhanced. These hHcys-induced EMT enhancement and Nox-dependent $O_2^{\cdot-}$/HIF-1α activation were significantly attenuated by rmGH treatment. HIF-1α level increased in Hcys-treated cultured podocytes, which were blocked by rmGH treatment. Meanwhile, homocysteine (Hcys)-induced EMT in cultured podocytes was significantly reversed by HIF-1α siRNA. All these results support the view that GH ameliorates hHcys-induced glomerular injury by reducing Nox-dependent $O_2^{\cdot-}$/HIF-1α signal pathway and EMT.

Keywords Homocysteine · Growth hormone · EMT · End-stage renal disease

C. Li · M. Xia · J. M. Abais · N. Li · K. M. Boini (✉) ·
P.-L. Li (✉)
Department of Pharmacology and Toxicology, Medical College
of Virginia Campus, Commonwealth University,
410 N, 12th Street, Richmond, VA 23298, USA
e-mail: kmboini@vcu.edu
e-mail: pli@vcu.edu

X. Liu
Division of Nephrology, Department of Internal Medicine; Tongji
Hospital, Tongji Medical College, Huazhong University of Science
and Technology, Wuhan, Hubei, People's Republic of China

Introduction

Increased plasma homocysteine (Hcys) level is well known to be associated with the progression of many degenerative diseases such as cardiovascular diseases, Alzheimer disease, and end-stage renal disease (ESRD) (Ravaglia et al. 2005; Sato et al. 2005; Moshal et al. 2006; Triantafyllou et al. 2008). With respect to ESRD, recent clinical studies have reported that plasma Hcys levels are associated with microalbuminuria, a predictive parameter of ESRD, which is independent of hypertension, diabetes mellitus, and cardiovascular disease (Francis et al. 2004; Sabanayagam and Shankar 2010). More recently, we and others have shown that nicotinamide adenine dinucleotide phosphate (NADPH) oxidase (Nox) activation and subsequent superoxide ($O_2^{\cdot-}$) production in podocytes are important early mechanisms in the development of hHcys-induced glomerular sclerosis (Sen et al. 2009; Yi et al. 2009b; Zhang et al. 2010a). Podocytes are an important structure of the glomerular filtration barrier. Increasing evidence indicates that podocytes may undergo epithelial-to-mesenchymal transition (EMT) upon various pathological stimuli causing functional

impairment, proteinuria, and glomerulosclerosis (Liu 2010; Boini et al. 2011b; Zhang et al. 2011). Our previous study showed that podocytes EMT enhancement could be regulated by redox signaling, while inhibition of $O_2^{\cdot-}$ production by knocking out the gene of an essential catalytic subunit of NADPH oxidase complex significantly blocked podocyte EMT (Zhang et al. 2011), indicating that treatment against Nox-derived oxidative stress would be a useful therapeutic strategy for hHcys-induced glomerular sclerosis. Interestingly, it has been shown that growth hormone exhibits anti-oxidative actions and that deficiency of growth hormone is involved in chronic kidney diseases (Wuhl and Schaefer 2002; Ungvari et al. 2010). Our recent in vitro study demonstrated that growth hormone (GH) reversed Hcys-induced podocytes EMT via inhibition of Nox-dependent $O_2^{\cdot-}$ production in cultured podocytes (Li et al. 2011). We wondered whether GH treatment would protect against the glomerular damage in vivo in hyperhomocysteinemia.

GH, a peptide hormone produced by the anterior pituitary, plays an important role in the regulation of renal function through increasing renal hemodynamics and filtration rate (Mak et al. 2008). It has been reported that GH resistance is involved in the progression of chronic kidney disease (CKD) and that treatment with recombinant GH can overcome GH resistant and improve the progression of CKD (Wuhl and Schaefer 2002). Moreover, recent studies have demonstrated that GH decreases oxidative stress and recover antioxidant defenses by reduction of reactive oxygen species (ROS) through various enzymatic pathways (Csiszar et al. 2008; Ungvari et al. 2010), which is consistent with our previous in vitro study (Li et al. 2011). Therefore, it is possible that GH may be involved in hHcys-induced glomerular injury.

It was reported recently that ROS induced epithelial cell EMT was mediated by hypoxia-inducible factor-1α (HIF-1α; Wu et al. 2012). HIF-1α has been demonstrated to be associated with the progression of chronic renal injuries (Nangaku 2006; Nangaku and Fujita 2008; Haase 2009). Our previous study showed HIF-1α contributes to the profibrotic action of angiotensin in renal medullary interstitial cells (Wang et al. 2011). However, whether HIF-1α is involved in signaling associated with podocytes EMT is not yet clear. The present study was to determine whether GH-mediated beneficial action would protect glomeruli from hHcys-induced injury through inhibition of ROS stimulated HIF-1α activation in vivo using an hHcys animal model.

We observed the beneficial effects of GH on hHcys-induced glomerular oxidative stress/HIF-1α activation, podocytes EMT, as well as glomerular damage in a mouse model, and also detected the effect of HIF-1α siRNA transfection on Hcys-induced EMT in cultured podocytes. Our results demonstrated that GH dramatically attenuated hHcys-induced activations of Nox-derived ROS and HIF-1α, and at the same time GH suppressed podocytes

EMT and glomerular sclerosis in hHcys, suggesting that GH is an important protective factor against hHcys-induced glomerular injury via the actions on ROS-induced HIF-1α activation and EMT.

Methods

Animal procedures

Male C57BL/6 J mice (8 weeks of age) were used. All protocols were approved by the Institutional Animal Care and Use Committee of Virginia Commonwealth University. To speed up the damaging effects of hHcys on glomeruli, all mice were uninephrectomized as we described previously (Yi et al. 2009b; Boini et al. 2011a) and others (Sen et al. 2009). This model has been demonstrated to induce glomerular damage unrelated to the uninephrectomy and arterial blood pressure, but specific to hHcys (Zhang et al. 2010b). After a 1-week recovery period from uninephrectomy, mice were fed a normal diet (ND) or a folate-free (FF) diet (Dyets Inc, Bethlehem, PA, USA) for 6 weeks with or without subcutaneous injection of rmGH (National Hormone & Peptide Program Harbor, UCLA Medical Center, Torrance, California, USA) at a dosage of 0.02 mg/kg, once a day. The dose of GH was chosen according to a recent report (Zhang et al. 2010d). One day before these mice were sacrificed, 24-h urine samples were collected using mouse metabolic cages. After blood samples were collected, these mice were sacrificed, and renal tissues were harvested for biochemical and molecular analysis as well as morphological examinations.

Cell culture

Conditionally immortalized mouse podocyte cell line, kindly provided by Dr. Klotman PE (Division of Nephrology, Department of Medicine, Mount Sinai School of Medicine, New York, NY, USA), were cultured on collagen I-coated flasks or plates in RPMI 1640 medium supplemented with recombinant mouse interferon-γ at 33 °C. After being differentiated at 37 °C for 10–14 days without interferon-γ, podocytes were used for the proposed experiments. In the present study, preparation of L-Hcys (a pathogenic form of Hcys) and rmGH, the concentration and the incubation time of L-Hcys and rmGH treatment were chosen based on our previous studies (Li et al. 2011).

ELISA analysis of GH level in plasma

The plasma GH levels were measured using a commercially available ELISA kit (R&D Systems, Minneapolis, MN, USA).

High-performance liquid chromatography analysis of plasma Hcys

Plasma total Hcys levels were measured by high-performance liquid chromatography (HPLC) method as we described previously (Chen et al. 2002).

Electromagnetic spin resonance analysis of Nox-dependent $O_2^{.-}$ production

For detection of Nox-dependent $O_2^{.-}$ production, proteins from the mouse renal cortex tissue were extracted using sucrose buffer and resuspended with modified Kreb's-Hepes buffer containing deferoximine (100 μmol/L, Sigma, St. Louis, MO, USA) and diethyl-dithiocarbamate (5 μmol/L, Sigma, St. Louis, MO, USA). The Nox-dependent $O_2^{.-}$ production was examined by addition of 1 mM NADPH as a substrate in 10 μg protein and incubated for 10 min at 37 °C in the presence or absence of SOD (200 U/ml), and then supplied with 1 mM $O_2^{.-}$-specific spin trap 1-hydroxy-3-methoxycarbonyl-2,2,5,5-tetramethylpyrrolidine (CMH, Noxygen, Elzach, Germany) as we described before (Yi et al. 2009b). The mixture was loaded in glass capillaries and immediately analyzed for $O_2^{.-}$ production kinetically for 10 min in a Miniscope MS200 electromagnetic spin resonance (ESR) spectrometer (Magnettech Ltd, Berlin, Germany). The ESR settings were as follows: biofield, 3350; field sweep, 60 G; microwave frequency, 9.78 GHz; microwave power, 20 mW; modulation amplitude, 3G; 4,096 points of resolution; and receiver gain, 20 for tissue and 50 for cells. The results were expressed as the fold changes vs. control.

Urinary total protein and albumin excretion measurement

Total protein content in 24-h urine samples was detected by Bradford method using a UV spectrophotometer. Urine albumin was detected by using a commercially available mouse albumin enzyme-linked immunoassay assay kit (Bethyl Laboratories, Montgomery, TX, USA) as we described previously (Zhang et al. 2010c).

Morphological examinations

For observation of renal morphology using light microscope, the kidneys were fixed with 4 % formalin solution, paraffin-embedded, and stained with periodic acid-Schiff. Glomerular sclerosis was assessed by a standard semiquantitative analysis and expressed as glomerular damage index (GDI; Iacobini et al. 2004). Fifty glomeruli per slide were counted and graded as 0, 1, 2, 3, or 4, according to 0, <25, 25–50, 51–75, or >75 % sclerotic changes cross a longitudinal kidney section, respectively. The GDI for each mouse was calculated by the formula: $(N_1 \times 1 + N_2 \times 2 + N_3 \times 3 + N_4 \times 4)/n$,

where N_1, N_2, N_3, and N_4 represent the numbers of glomeruli exhibiting injury grades 1, 2, 3, and 4, respectively, and n is the total number of glomeruli graded.

Immunofluorescent staining

Immunofluorescent staining was performed using frozen slides of mouse kidneys. After fixation with acetone, the slides were incubated with antibodies against podocin at 1:200 (Sigma, St. Louis, MO, USA) or desmin at 1:100 (BD Biosciences, San Jose, CA, USA) overnight at 4 °C. Then, the slides were washed and incubated with corresponding Texas Red or Green-labeled secondary antibodies. Finally, the slides were washed, mounted, and subjected to fluorescent microscopic examinations. The images were captured with a spot charge-coupled device camera. All exposure settings were kept constant for each group of kidneys (Boini et al. 2010).

The cells slides were fixed in 4 % PFA for 15 min. After rinsing with phosphate-buffered saline (PBS), cells were incubated with goat anti-FSP-1 (1: 50, Santa Cruz Biotechnology, Inc, Santa Cruz, CA, USA), goat anti-P-cadherin (1: 50, R&D system, Minneapolis, MN, USA) antibodies. After washing, the slides were incubated with Alex-488-labeled secondary antibodies for 1 h at room temperature. After mounting with DAPI-containing mounting solution, the slides were observed under a fluorescence microscope under which photos were taken and analyzed.

Double-immunofluorescent staining and confocal microscopy

Double-immunofluorescent staining was performed using frozen slides from mouse kidneys. After fixation with acetone, the slides were incubated with rabbit antipodocin or antidesmin antibody at 1:50 (Sigma), which was followed by the incubation with Alex-555-labeled goat antirabbit secondary antibody. Then, goat FSP-1 antibody at 1:50, goat anti-zona occludens 1 (ZO-1) antibody at 1: 25 (Santa Cruz Biotechnology Inc), goat anti-P-cadherin antibody at 1:25, mouse anti-α smooth muscle actin (α-SMA) antibody at 1:200 (R&D system, Minneapolis, MN, USA), or goat antigrowth hormone receptor 1:50 (Sigma, St. Louis, MO, USA) was used to incubate the slides for overnight at 4 °C. In addition, colocalization of P-cadherin vs. ZO-1 (Invitrogen) and FSP-1 vs. α-SMA was observed in the slides of same groups. After washing, the slides were incubated with corresponding Alex-488-labeled secondary antibodies. Finally, the slides were mounted and subjected to examinations using a confocal laser scanning microscope (Fluoview FV1000, Olympus, Japan; Boini et al. 2011a)

Real-time reverse transcription polymerase chain reaction

Total RNA from renal cortex tissue was extracted using TRIzol reagent (Invitrogen, Carlsbad, CA, USA) according to the protocol as described by the manufacturer. Aliquots of total RNA (1 μg) from each sample were reverse-transcribed into cDNA according to the instructions of the first strand cDNA synthesis kit manufacturer (Bio-Rad, Hercules, CA, USA). Equal amounts of the reverse transcriptional products were subjected to polymerase chain reaction (PCR) amplification using SYBR Green as the fluorescence indicator on a Bio-Rad iCycler system (Bio-Rad). The mRNA levels of target genes were normalized to the β-actin mRNA levels. The primers used in this study were synthesized by Operon (Huntsville, AL, USA) and the sequences were: P-cadherin sense GTAAGGGCTACCGCT CACTC, antisense TGTGAGGCCAAGTGAAAGAC; ZO-1 sense GAGCTACGCTTGCCACACTGT, antisense TCGGATCTCCAGGAAGACACTT; FSP-1 sense GTTACCATGGCAAGACCCTT, antisense AACTTGTCA CCCTCTTTGCC; α-SMA sense CAGGATGCAGAAGGA GATCA, antisense TCCACATCTGCTGGAAGGTA; growth hormone receptor: sense CCUCCAUUUGGAUAC CCUAUU, antisense UAGGGUAUCCAAAUGGAGGTA; podocin sense TGGCACATCGATCCCTCACTGAAA, antisense AGGTCACTGCAT CTAAGGCAACCT; desmin sense CAGTCCTACACCTGCGAGATT, antisense GGCCAT CTTCACATTGAGC; β-actin sense TCGCTGC GCTGGTCGTC, antisense GGCCTC GTCACCCACATA GGA (Li et al., 2011).

Western blot analysis

Nuclear protein or homogenates preparation and the complete protocol for Western blot analysis have been described previously (Li et al. 2007). The primary antibodies used in this study are antipodocin (1:1,000, Sigma), antidesmin (1:1,000, BD Biosciences), anti-ZO-1 (1:500, Invitrogen), anti-P-cadherin (1:500, R&D System), anti-α-SMA (1:5,000, R&D System), anti-FSP-1 (1:1,000, Abcam), anti-HIF-1α (1:500, Novus Biologicals, Littleton, CO, USA) or anti-β-actin (1:10,000, Santa Cruz Biotechnology).

Transfection of HIF-1α siRNA

Transfection of siRNA was performed using the siLentFect lipid reagent (Bio-Rad) according to the manufacturer's instructions. For a 10-cm dish, 200 pmol of siRNA was used. After 6-h incubation in transfection reagent, the cells were then switched to normal medium for overnight recovery and ready for experiment. The target sequence of HIF-1α siRNA was: CCGCTCAATTTATGAATATTA (QIAGEN, Valencia, CA, USA). A scrambled siRNA (QIAGEN),

which was confirmed as nonsilencing double-stranded RNA, was used as control for siRNA experiments.

Statistical analysis

All of the values were expressed as mean±SEM. Significant differences among multiple groups were examined using ANOVA followed by a Student–Newman–Keuls test. χ^2 test was used to assess the significance of ratio and percentage data. $p < 0.05$ was considered statistically significant.

Results

Changes in plasma GH level and glomerular growth hormone receptor expression in hHcys mice

We detected the plasma GH levels in control and hHcys mice with or without rmGH treatment. It was found that GH level were significantly reduced in hHcys mice and the reduced GH was restored by rmGH treatment (Fig. 1a). Real-time PCR data showed that glomerular growth hormone receptor (GHR) mRNA level was significantly increased by 1.57-fold in hHcys mice compared with control mice. However, these increased renal GHR mRNA expression in hHcys mice was substantially attenuated by rmGH treatment (Fig. 1b). Immunofluorescent analysis showed that GHR staining was more pronounced in the glomeruli of hHcys mice compared with control mice and that rmGH treatment decreased the elevation of GHR expression in hHcys mice (Fig. 1c). There was no significant difference in GHR expression in the glomeruli from control mice with or without rmGH treatment. The summarized data are shown in Fig. 1d.

Improvement of glomerular injury by rmGH treatment in hHcys mice

HPLC analysis revealed that FF diet treatment significantly increased the plasma total Hcys levels in uninephrectomized C57BL/6 J mice compared with ND mice. The treatment of rmGH did not change the Hcys levels (Table 1). In parallel to the elevation of the plasma total Hcys level, urinary volume, total protein, and albumin excretion were significantly increased in hHcys mice compared with control mice (Fig. 2a, b; Table 1). However, rmGH treatment significantly attenuated the increases in urinary total protein and albumin excretion (Fig. 2a, b) in hHcys mice. Morphological analysis showed a typical pathological change in glomerular sclerotic damage, such as hypercelluarity, capillary collapse, and extracellular matrix deposition in hHcys mice. The average glomerular damage index was significantly higher in hHcys mice. Treatment with rmGH attenuated this
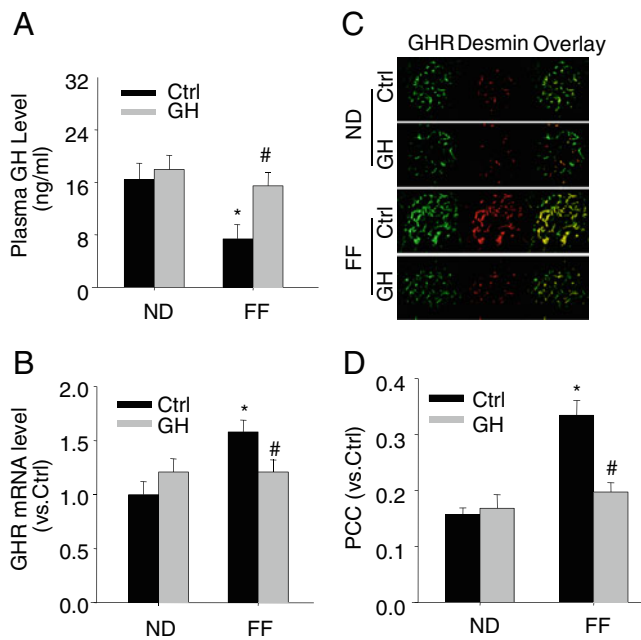
Fig. 1 Plasma GH level, mRNA and protein level of GHRs in glomeruli of mice on normal diet or FF diet with or without GH treatment. **a** ELISA data of GH level in mice plasma ($n=6$/group). **b** Real-time PCR analysis of GHR mRNA expression. The data are presented as the fold changes compared with mice on the normal diet ($n=7$/group). **c** Representative confocal fluorescent images for GHR and desmin in glomeruli from different mice. **d** Summarized co-localization coefficient data showing co-localization levels of desmin and GHR in different groups of mice ($n=4$/group). *$p<0.05$ vs. mice on the normal group, #$p<0.05$ vs. vehicle-treated mice on hHcys group

hHcys-induced glomerular injury in mice (Fig. 2c, d). The growth hormone treatment did not alter the body weight in control or FF diet fed mice with or without growth hormone treatment. We also found that growth hormone treatment did not cause mortality in ND or FF diet fed mice (Table 1).

Protective role of rmGH on the podocyte injury in hHcys mice

We tested the effect of rmGH on the levels of podocin and desmin, which were used as indications of podocyte damage. It was found that the mRNA and protein levels of

podocin, a podocyte marker, were significantly decreased in hHcys mice. Treatment with rmGH significantly attenuated the hHcys-induced such podocin decrease (Fig. 3a–c). In contrast, mRNA and protein levels of desmin, a podocyte injury marker, were significantly increased in hHcys mice, which were significantly inhibited by rmGH treatment (Fig. 3e–g). Immunofluorescent analysis showed that podocin staining was expressed as a fine linear-like pattern along the glomerular capillary loop. The podocin staining dramatically decreased in the glomeruli from hHcys mice compared with control mice. RmGH treatment restored this hHcys-induced podocin decrease in the glomeruli (Fig. 3d). Desmin was less stained in the glomerular capillary loop on the control mice, which was markedly increased in hHcys mice. RmGH treatment almost abolished the increase of desmin staining in glomeruli (Fig. 3h).

Immunofluorescent analysis of EMT markers in the glomeruli

Figure 4a showed the podocyte phenotypic changes upon hHcys with or without rmGH treatment by immunofluorescent staining, where red color represented podocyte marker podocin expression and green represented EMT markers expression in glomeruli. Colocalization of epithelial markers (P-cadherin and ZO-1) with podocin were significantly decreased in the glomeruli from hHcys mice compared with control mice. RmGH injection substantially recovered this hHcys-induced decrease in the expression of epithelial markers and podocin. However, Fig. 4b showed mesenchymal markers, FSP-1 and α-SMA were very weak in the glomeruli from control mice, while mesenchymal markers expression significantly increased in the glomeruli from hHcys mice. This hHcys-induced increase of mesenchymal markers was markedly inhibited by rmGH treatment.

Protective effect of rmGH on EMT markers expression in renal cortex of hHcys mice

To further determine the role of rmGH against EMT in the glomeruli, we detected the effect of rmGH on the mRNA

Table 1 Body weight, plasma Hcys concentration, and urine volume in C57BL/6J WT mice fed a ND or FF diet with or without growth hormone treatment ($n=5–11$)

Parameters	Ctrl ND	GH ND	Ctrl FF	GH FF
Body weight (g)	22.8±1.0	22.5±0.8	23.9±1.5	23.5±1.2
Hcys conc (μM)	4.5±0.5	4.3±0.5	58.1±8.4[*]	54.7±8.8[*]
Urine volume (ml)	0.5±0.1	0.7±0.1	1.2±0.1[*]	1.2±0.2[*]

The data was expressed as mean±SEM

ND normal diet, *FF* folate-free diet, *GH* growth hormone, *Hcys* homocysteine

[*] $p<0.05$ as compared with Vehi ND
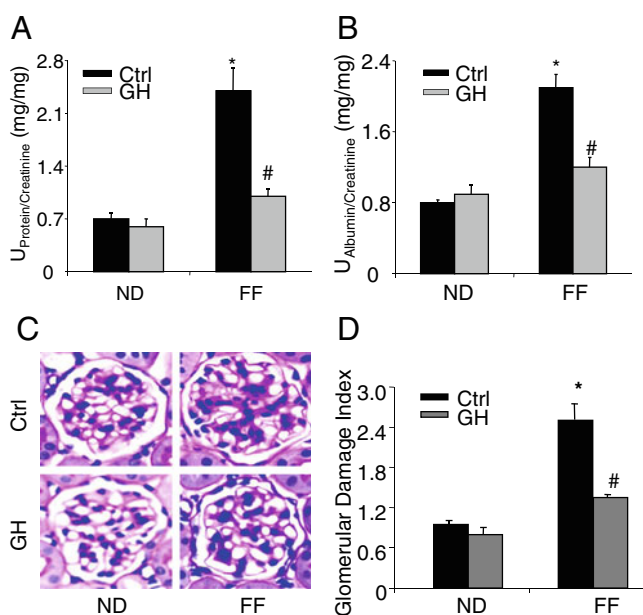
Fig. 2 Urinary protein, albumin excretion and morphological features of glomeruli in C57BL/6J mice on the normal diet or folate free diet with or without GH treatment. **a** Urinary total protein excretion of mice on the normal diet or folate free diet with or without GH treatment (n=8–11/group). **b** Urinary albumin excretion (n=9–11/group). **c** Photomicrographs show typical glomerular structure (original magnification, ×400; n=6 /group). **d** Summarized data of glomerular damage index (GDI) by semiquantitation of scores in four different groups of mice. For each kidney section, 50 glomeruli were randomly chosen for calculation of GDI. *p<0.05 vs. mice on the normal group, #p<0.05 vs. vehicle-treated mice on hHcys group

and protein levels of epithelial markers, P-cadherin and ZO-1. As shown in Fig. 5a, the mRNA levels of P-cadherin and ZO-1 were significantly decreased to 77 and 70 % in the cortex of hHcys mice, which were recovered by rmGH injection. Figure 5b showed the protein expression of these two epithelial markers presented a similar tendency like mRNA levels. However, rmGH had no significant effects in the protein and mRNA levels of p-cadherin and ZO-1 in normal diet-fed mice. The summarized data of protein expression are presented in Fig. 5c.

We also determined the effect of rmGH on the expression of mesenchymal markers, α-SMA and FSP-1 in the renal cortex. As depicted in Fig. 5d and e, the α-SMA and FSP-1 protein levels and α-SMA mRNA level significantly increased in hHcys mice compared with control mice. The mRNA level of FSP-1 was also found to be increased in hHcys mice, which also had a tendency to decrease although it did not reach statistical significance (Fig. 5d, p=0.07). RmGH treatment significantly inhibited the increases in these hHcys-induced mesenchymal markers. Similar to its actions on epithelial markers, rmGH had no evident effects in protein and mRNA expression of α-SMA and FSP-1 in normal diet-fed mice. The summarized data of protein expression are presented in Fig. 5f.
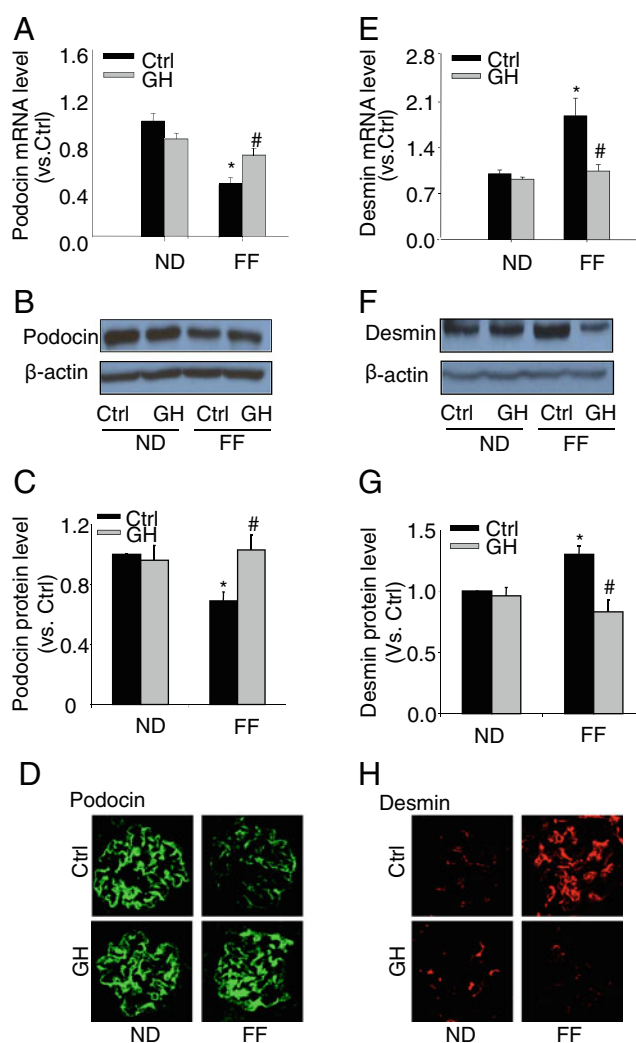
Fig. 3 Effects of GH on hHcys-induced changes in mRNA and protein expression of podocin and desmin in glomeruli from mice on the normal diet or FF diet. **a** Real-time PCR analysis of podocin mRNA level in the glomeruli of different groups of mice (n=6–7/group). **b** Western blot analysis of podocin protein expression (n=6/group). **c** Summarized data of podocin protein density. **d** Typical images of podocin staining in glomeruli (n=4/group). **e** Real-time PCR analysis of desmin mRNA expression in the glomeruli of different groups of mice (n=5–7/group). **f** Western blot analysis of desmin protein expression (n=5/group). **g** Summarized data of desmin protein density. **h** Typical images of desmin staining in glomeruli (n=4/group). *p<0.05 vs. mice on the normal group, #p<0.05 vs. vehicle-treated mice on hHcys group

Treatment of rmGH decreased $O_2^{\cdot-}$ and HIF-1α level in the renal cortex of hHcys mice

To explore the potential mechanism underlying rmGH recovery of glomerular injury, we determined NADPH-oxidase-dependent $O_2^{\cdot-}$ production in the renal cortex. As shown in Fig. 6a and b, ESR analysis demonstrated that Nox-derived $O_2^{\cdot-}$ production was significantly increased in hHcys mice compared with control mice. RmGH treatment markedly attenuated this hHcys-induced increase in $O_2^{\cdot-}$
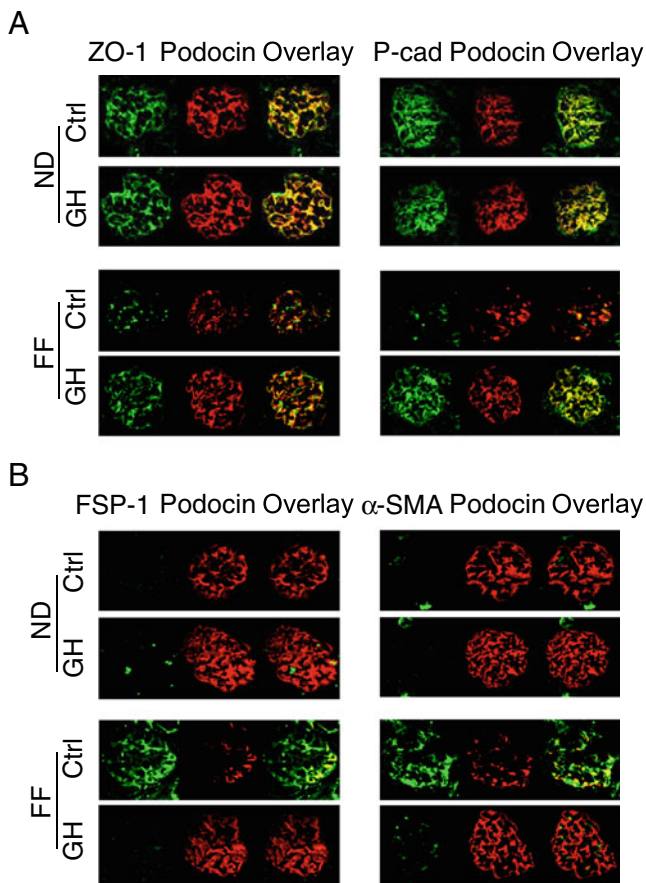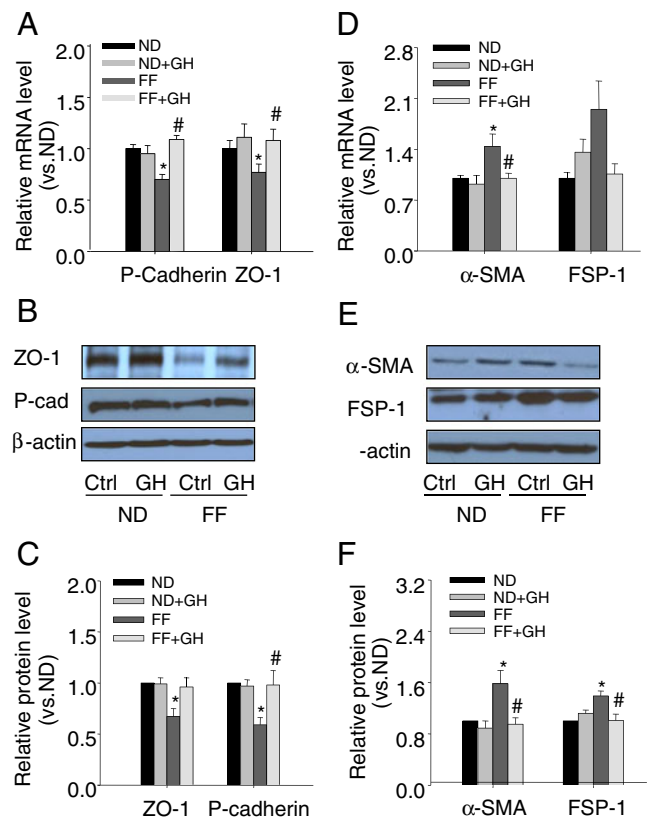
Fig. 4 Immunofluorescent staining of EMT markers in glomeruli from mice on the normal diet or FF diet with or without GH treatment. **a** Typical confocal microscopic results of Podocin vs. ZO-1 or P-cadherin staining in glomeruli from mice on the normal diet or FF diet with or without GH treatment (*n*=4/group). **b** Typical confocal microscopic results of podocin vs. FSP-1 or α-SMA staining in glomeruli from mice, respectively (*n*=4/group)

Fig. 5 GH inhibited hHcys-induced podocytes EMT in glomeruli from different groups of mice. **a** Real-time PCR analysis of ZO-1 and P-cadherin mRNA expression in glomeruli of different groups of mice (*n*=6–7/group). **b** Western blot analysis of ZO-1 and P-cadherin protein expression in different groups of mice (*n*=5–7/group). **c** Summarized data of ZO-1 and P-cadherin density. **d** Real-time PCR analysis of α-SMA and FSP-1 mRNA expression in glomeruli of different groups of mice (*n*=6–7/group). **e** Western blot analysis of α-SMA and FSP-1 protein expression in different groups of mice. **f** Relative quantitation of protein expression for Western blot analysis from different groups of mice (*n*=6/group). *$p<0.05$ vs. mice on the normal group, #$p<0.05$ vs. vehicle-treated mice on hHcys group

production. However, rmGH treatment had no significant effect on glomerular $O_2^{\cdot-}$ production in control mice.

HIF-1α, one of the major factors mediating EMT, has been implicated in chronic renal injury and that HIF-1α can be increased by ROS, we detected whether rmGH treatment also reduced hHcys-induced HIF-1α increases. Our results demonstrated that hHcys alone significantly increases HIF-1α protein levels in vivo (Fig. 6c, d). However, rmGH treatment blocked hHcys-induced HIF-1α increases. RmGH treatments alone did not show any effect on the HIF-1α protein levels in vivo.

HIF-1α siRNA blocked Hcys-induced EMT in cultured podocytes

To determine the role of HIF-1α in Hcys-induced podocyte EMT, we examined whether inhibition of HIF-1α would block the Hcys-induced EMT. As shown in Fig. 7a and b, Hcys induced HIF-1α in cultured podocytes. However, in the cells

transfected with HIF-1α siRNA, hHcys-induced decreases in epithelial marker, p-cadherin was significantly reversed (Fig. 7c). The fold changes of the P-cadherin in different cultured cells were summarized in Fig. 7d. Using immunofluorescent staining, Fig. 7e further confirmed that inhibition of HIF-1α expression with HIF-1α siRNA reversed the Hcys-induced changes in P-cadherin and FSP-1 expression.
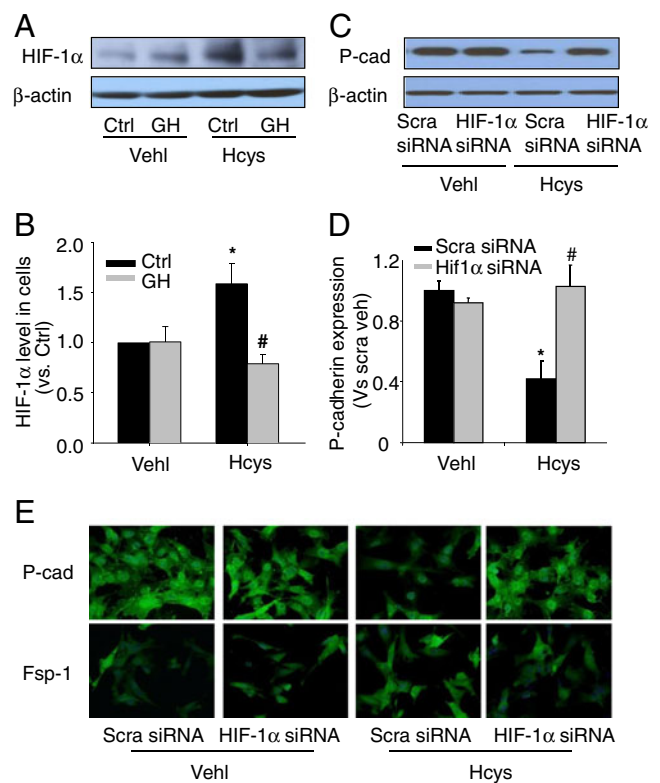
Discussion

The present study demonstrated that plasma GH level was significantly decreased in hHcys mice. RmGH treatment recovered the GH levels and attenuated the hHcys-induced activation of ROS/HIF-1α signal pathway and improved the kidney damage. A novel finding of our study is that GH treatment reduced the upregulation of mesenchymal markers
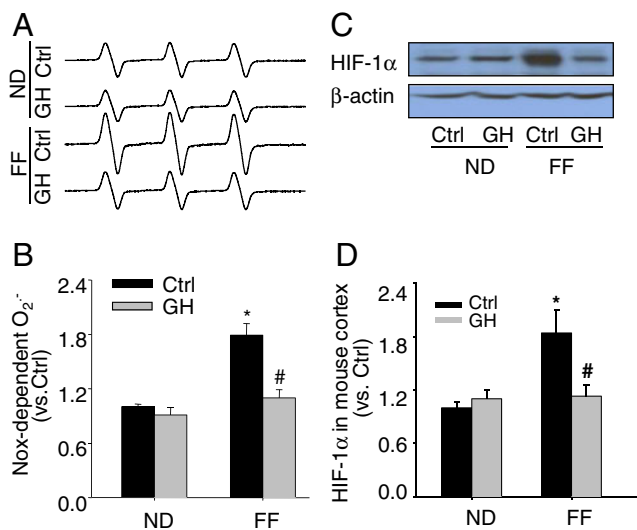
Fig. 6 GH reduced hHcys-induced Nox-dependent $O_2^{\cdot-}$ and HIF-1α level in renal cortex tissue. **a** Representative ESR spectra traces for Nox-dependent $O_2^{\cdot-}$ production in the cortex from mice on a normal diet or FF diet with or without GH treatment. **b** Summarized data show fold changes in Nox-dependent $O_2^{\cdot-}$ production, which are normalized to vehicle-treated mice on the normal diet under different conditions ($n=6$/ group). $O_2^{\cdot-}$ was measured by ESR with a trapping substance for SOD-sensitive $O_2^{\cdot-}$. **c** Western blot analysis of HIF-1α level in different groups of mice. **d** Relative quantitation of protein expression for Western blot analysis from different groups of mice ($n=6$/group). *$p<0.05$ vs. mice on the normal group, #$p<0.05$ vs. vehicle-treated mice on hHcys group

Fig. 7 Effect of rmGH on hHcy-induced increases in HIF-1α production in podocytes and HIF-1siRNA blocked hHcy-induced podocytes EMT. **a** Western blot analysis of HIF-1α expression in different groups of mice. **b** Relative quantitation of protein expression for Western blot analysis from different groups of cell ($n=5$/group). **c** Western blot analysis of P-cadherin expression in different groups of cells. **d** Summarized data of P-cadherin protein density ($n=5$/group). **e** Representative images show the expression of P-cadherin and FSP-1 as epithelial marker and mesenchymal marker in different groups ($n=5$/ group).*$p<0.05$ vs. podocyte on the normal group, #$p<0.05$ vs. vehicle-treated podocyte on hHcys group

and rescued the decrease of epithelial markers. Our results demonstrate for the first time that GH treatment attenuated kidney injury by blocking EMT through inhibiting the activations of Nox-dependent $O_2^{\cdot-}$/HIF-1α pathway in hHcys. To our knowledge, the present study for the first time report that GH treatment in mice prevents glomerular injury induced by hHcys in vivo study.

The GH system is present in the kidney and is important to kidney structure and function. GH-induced biological responses are mainly associated with its binding to GHRs. It has been reported that GH level may be decreased, normal, or even increased in CKD (Feneberg et al. 2003). Our data shows that GH level in plasma were significantly decreased and GHR expression in glomeruli was significantly increased in the hHcys mice compared with control mice, while GH treatment recovered the plasma GH level and inhibited this hHcys-associated GHR upregulation. The upregulation of GHR may be due to the feedback effect of reduced GH levels. This is consistent with a recently report that showed GH induced GHR downregulation (Deng et al. 2012). Colocalization of GHR with desmin in the present study indicates that GHR is also located in podocytes, which is consistent with our previous in vitro study showing that GH protected podocyte from Hcys-induced damage (Li et al. 2011). These results suggest that hHcys-induced glomerular injury is associated with a reduced GH level in the

plasma and abnormal GHR expression in the glomeruli, and that normalization of the GH system may exhibit beneficial effects in chronic renal injury in hHcys.

RmGH treatment significantly attenuated hHcys-induced increase of the urinary protein, albumin excretion, and glomerular pathological injuries. These results suggest that administration of GH may prevent hHcys-induced glomerular injury and therefore the maintenance of normal GH level may be important for the protection of kidneys from hHcys-induced injury or sclerosis. There are some evidences that GH treatment reverses early atherosclerotic changes in growth hormone deficient adults (Pfeifer et al. 1999) or possess significant cardiac protective effect in uremia rats (Krieg et al. 2008; Rabkin et al. 2008). In addition, GH-releasing peptide ghrelin has recently been reported to protect the endothelium from Hcys-induced injury, which is associated with increases in endothelial nitric oxide synthase expression and reduction of oxidative stress (Hedayati et al. 2009). These reports in combination with the results from the present study

suggest that GH treatment may protect multiple organs against hHcys-induced damages including the kidneys. Because reduced GH levels or insensitive to GH occurs in other types of chronic kidney diseases, the GH treatment may also produce beneficial effects in chronic renal injury other than hHcys, which requires further investigation. Given the anabolic properties of GH and its effects on increasing protein synthesis and muscle mass, the earlier studies have investigated the relationship of growth hormone and plasma homocysteine concentration in patients. In a randomized-controlled trial by Sesmilo et al. (2001), it is reported that GH treatment for 18 months declined plasma Hcys levels by 0.6 μM compared to placebo-treated patients. In contrast, another two studies failed to confirm the correlation of growth hormone and plasma Hcys levels (Lewandowski et al. 2003; Randeva 2003). Indeed, our results did not find difference in plasma Hcys levels in animals treated with or without rmGH, indicating that the beneficial effect of GH is not due to its involvement in the metabolism of Hcys.

To explore the mechanism mediating the protective action of GH on glomerular injury in hHcys, we observed the changes in podocyte damage during hHcys, given that podocyte dysfunction or effacement is considered the initiating mechanism to produce glomerular injury or sclerosis, leading to proteinuria with possible progression to ESRD (Dressler 2006; Leeuwis et al. 2010). The present study showed that podocin expression was reduced in the glomeruli of hHcys mice at both protein and mRNA level, while another podocyte injury marker, desmin was significantly increased in hHcys mice, which was abolished by rmGH treatment. These results were consistent with our previous reports in cultured podocytes that GH recovered Hcy-induced podocyte injury through inhibited cell EMT phenotype (Li et al. 2011). The current study also showed that GH inhibited glomerular EMT process in hHcys animal model. These changed EMT markers were colocalized with podocyte marker such as podocin, indicating that EMT changes in glomeruli of hHcys mice indeed occurred in podocytes. Since EMT is critically involved in the initiation and development of glomerular sclerosis (Kang et al. 2010), the blocking action of GH on glomerular EMT may be an important mechanism to protect glomeruli from hHcys-induced injury.

We also determined the possible inhibitory effect on local oxidative stress by GH on glomerular injury in mice with hHcys. These studies were focused on GH possible inhibitory effect on local oxidative stress, because previous studies demonstrated that GH had beneficial effect on oxidative stress-associated injury in other tissues or organs such as heart, vessels, and lymphocytes (Arnold and Weigent 2003; Seiva et al. 2008; Ungvari et al. 2010). At the same time, our previous studies demonstrated that Hcys-induced Nox-derived $O_2^{\cdot-}$ production and subsequent injury of different types of renal glomerular cells including podocytes (Yi et al. 2009a; Zhang et al. 2010a). The present study showed that hHcys significantly increased Nox-dependent $O_2^{\cdot-}$ production in glomeruli and such $O_2^{\cdot-}$ production was substantially inhibited by rmGH treatment. It is suggested that GH may exerts its protective action via suppression of $O_2^{\cdot-}$ production in glomeruli.

Although increased ROS production in response to hHcys has been demonstrated to be involved in hHcys-induced podocytes EMT (Li et al. 2011; Zhang et al. 2011), the downstream pathway of ROS has not been determined in hHcys. HIF-1α, a key mediator of cellular adaptation to hypoxia, has been reported to induce EMT through direct regulation of Twist, which inhibits epithelial marker transcription (Yang and Wu 2008; Yang et al. 2008; Sun et al. 2009; Zhu et al. 2011). It has also been demonstrated that ROS production contributed to HIF1-α activation (Griguer et al. 2006; Wu et al. 2012). Our data in the present study showed that hHcys significantly increased the HIF-1α levels in vitro and in vivo, while knocking down of HIF-1α totally abolished this hHcys-induced EMT phenotype in podocytes, providing further evidence that HIF-1α, as an important positive regulator of EMT, critically involved in the hHcys-induced podocyte EMT.

One interesting finding in this study is that GH level in hHcys mice is significantly decreased while GHR expression was increased compared with control mice. The reason for a low level of GH in hHcys mice is probably that activated HIF-1α inhibited GH expression, which increased GHR expression by the negative feedback loop. HIF-1α regulates many target genes and thereby has an important role in many physiological processes (Wang et al. 2011). Recent study has shown that HIF-1 α may directly bind to GH promoter region and decreased GH mRNA level (Vakili et al. 2012). It has also been reported that overexpression of HIF-1α or exposure to the hypoxia mimetic CoCl2 significantly increase GHR mRNA levels and its promoter activities (Erman et al. 2011). These reports are consistent with our present study, which showed that rmGH treatment reduced the HIF-1α levels and the GHR expression in hHcys mice. Taken together, our data suggest that rmGH treatment inhibited the hHcys-induced EMT phenotype through ROS/HIF-1α signaling pathway.

In summary, the present study demonstrated a beneficial action of GH on hHcys-induced glomerular injury, which was attributed to its inhibition of glomeruli EMT via suppressing ROS/HIF-1α signal pathway. It is concluded that GH may be a novel therapeutic reagent for the prevention and treatment of hHcys-induced glomerular injury or sclerosis.

References

Arnold RE, Weigent DA (2003) The inhibition of superoxide production in EL4 lymphoma cells overexpressing growth hormone. Immunopharmacol Immunotoxicol 25:159–177

Boini KM, Xia M, Li C, Zhang C, Payne LP, Abais JM, Poklis JL, Hylemon PB, Li PL (2011a) Acid sphingomyelinase gene deficiency ameliorates the hyperhomocysteinemia-induced glomerular injury in mice. Am J Pathol 179(5):2210–2219

Boini KM, Xia M, Xiong J, Li C, Payne LP, Li PL (2011b) Implication of CD38 gene in podocyte epithelial-to-mesenchymal transition and glomerular sclerosis. J Cell Mol Med 6(8):1674–1685

Boini KM, Zhang C, Xia M, Poklis JL, Li PL (2010) Role of sphingolipid mediator ceramide in obesity and renal injury in mice fed a high-fat diet. J Pharmacol Exp Ther 334:839–846

Chen YF, Li PL, Zou AP (2002) Effect of hyperhomocysteinemia on plasma or tissue adenosine levels and renal function. Circulation 106:1275–1281

Csiszar A, Labinskyy N, Perez V, Recchia FA, Podlutsky A, Mukhopadhyay P, Losonczy G, Pacher P, Austad SN, Bartke A, Ungvari Z (2008) Endothelial function and vascular oxidative stress in long-lived GH/IGF-deficient Ames dwarf mice. Am J Physiol Heart Circ Physiol 295:H1882–H1894

Deng L, Jiang J, Frank SJ (2012) Growth hormone-induced JAK2 signaling and GH receptor down-regulation: role of GH receptor intracellular domain tyrosine residues. Endocrinology 153(5):2311–2322

Dressler GR (2006) The cellular basis of kidney development. Annu Rev Cell Dev Biol 22:509–529

Erman A, Wabitsch M, Goodyer CG (2011) Human growth hormone receptor (GHR) expression in obesity: II. Regulation of the human GHR gene by obesity-related factors. Int J Obes (Lond) 35:1520–1529

Feneberg R, Schaefer F, Veldhuis JD (2003) Neuroendocrine adaptations in renal disease. Pediatr Nephrol 18:492–497

Francis ME, Eggers PW, Hostetter TH, Briggs JP (2004) Association between serum homocysteine and markers of impaired kidney function in adults in the United States. Kidney Int 66:303–312

Griguer CE, Oliva CR, Kelley EE, Giles GI, Lancaster JR Jr, Gillespie GY (2006) Xanthine oxidase-dependent regulation of hypoxia-inducible factor in cancer cells. Cancer Res 66:2257–2263

Haase VH (2009) Pathophysiological consequences of HIF activation: HIF as a modulator of fibrosis. Ann N Y Acad Sci 1177:57–65

Hedayati N, Annambhotla S, Jiang J, Wang X, Chai H, Lin PH, Yao Q, Chen C (2009) Growth hormone-releasing peptide ghrelin inhibits homocysteine-induced endothelial dysfunction in porcine coronary arteries and human endothelial cells. J Vasc Surg 49:199–207

Iacobini C, Menini S, Oddi G, Ricci C, Amadio L, Pricci F, Olivieri A, Sorcini M, Di Mario U, Pesce C, Pugliese G (2004) Galectin-3/AGE-receptor 3 knockout mice show accelerated AGE-induced glomerular injury: evidence for a protective role of galectin-3 as an AGE receptor. FASEB J 18:1773–1775

Kang YS, Li Y, Dai C, Kiss LP, Wu C, Liu Y (2010) Inhibition of integrin-linked kinase blocks podocyte epithelial-mesenchymal transition and ameliorates proteinuria. Kidney Int 78:363–373

Krieg RJ Jr, Veldhuis JD, Thornhill BA, Chevalier RL, Gil G (2008) Growth hormone (GH) secretion, GH-dependent gene expression, and sexually dimorphic body growth in young rats with chronic renal failure. Endocrine 33:323–330

Leeuwis JW, Nguyen TQ, Dendooven A, Kok RJ, Goldschmeding R (2010) Targeting podocyte-associated diseases. Adv Drug Deliv Rev 62:1325–1336

Lewandowski KC, Murray RD, Drzewoski J, O'Callaghan CJ, Czupryniak L, Hillhouse EW, Shalet SM, Randeva HS (2003) Plasma total homocysteine concentrations in adults with growth hormone (GH) deficiency: effects of GH replacement. Mol Genet Metab 80:330–337

Li CX, Xia M, Han WQ, Li XX, Zhang C, Boini KM, Liu XC, Li PL (2011) Reversal by growth hormone of homocysteine-induced epithelial-to-mesenchymal transition through membrane raft-redox signaling in podocytes. Cell Physiol Biochem 27:691–702

Li N, Yi F, Sundy CM, Chen L, Hilliker ML, Donley DK, Muldoon DB, Li PL (2007) Expression and actions of HIF prolyl-4-hydroxylase in the rat kidneys. Am J Physiol Renal Physiol 292:F207–F216

Liu Y (2010) New insights into epithelial-mesenchymal transition in kidney fibrosis. J Am Soc Nephrol 21:212–222

Mak RH, Cheung WW, Roberts CT Jr (2008) The growth hormone-insulin-like growth factor-I axis in chronic kidney disease. Growth Horm IGF Res 18:17–25

Moshal KS, Singh M, Sen U, Rosenberger DS, Henderson B, Tyagi N, Zhang H, Tyagi SC (2006) Homocysteine-mediated activation and mitochondrial translocation of calpain regulates MMP-9 in MVEC. Am J Physiol Heart Circ Physiol 291:H2825–H2835

Nangaku M (2006) Chronic hypoxia and tubulointerstitial injury: a final common pathway to end-stage renal failure. J Am Soc Nephrol 17:17–25

Nangaku M, Fujita T (2008) Activation of the renin-angiotensin system and chronic hypoxia of the kidney. Hypertens Res 31:175–184

Pfeifer M, Verhovec R, Zizek B, Prezelj J, Poredos P, Clayton RN (1999) Growth hormone (GH) treatment reverses early atherosclerotic changes in GH-deficient adults. J Clin Endocrinol Metab 84:453–457

Rabkin R, Awwad I, Chen Y, Ashley EA, Sun D, Sood S, Clusin W, Heidenreich P, Piecha G, Gross ML (2008) Low-dose growth hormone is cardioprotective in uremia. J Am Soc Nephrol 19:1774–1783

Randeva HS (2003) Hormonal regulation of homocysteine. Metab Syndr Relat Disord 1:121–128

Ravaglia G, Forti P, Maioli F, Martelli M, Servadei L, Brunetti N, Porcellini E, Licastro F (2005) Homocysteine and folate as risk factors for dementia and Alzheimer disease. Am J Clin Nutr 82:636–643

Sabanayagam C, Shankar A (2010) Association between plasma homocysteine and microalbuminuria in persons without hypertension, diabetes mellitus, and cardiovascular disease. Clin Exp Nephrol 15(1):92–99

Sato Y, Honda Y, Iwamoto J, Kanoko T, Satoh K (2005) Effect of folate and mecobalamin on hip fractures in patients with stroke: a randomized controlled trial. JAMA 293:1082–1088

Seiva FR, Ebaid GM, Castro AV, Okoshi K, Nascimento A, Rocha KK, Padovani CR, Cicogna AC, Novelli EL (2008) Growth hormone and heart failure: oxidative stress and energetic metabolism in rats. Growth Horm IGF Res 18:275–283

Sen U, Basu P, Abe OA, Givvimani S, Tyagi N, Metreveli N, Shah KS, Passmore JC, Tyagi SC (2009) Hydrogen sulfide ameliorates hyperhomocysteinemia-associated chronic renal failure. Am J Physiol Renal Physiol 297:F410–F419

Sesmilo G, Biller BM, Llevadot J, Hayden D, Hanson G, Rifai N, Klibanski A (2001) Effects of growth hormone (GH) administration on homocyst(e)ine levels in men with GH deficiency: a randomized controlled trial. J Clin Endocrinol Metab 86:1518–1524

Sun S, Ning X, Zhang Y, Lu Y, Nie Y, Han S, Liu L, Du R, Xia L, He L, Fan D (2009) Hypoxia-inducible factor-1alpha induces Twist expression in tubular epithelial cells subjected to hypoxia, leading to epithelial-to-mesenchymal transition. Kidney Int 75:1278–1287

Triantafyllou N, Evangelopoulos ME, Kimiskidis VK, Kararizou E, Boufidou F, Fountoulakis KN, Siamouli M, Nikolaou C, Sfagos C, Vlaikidis N, Vassilopoulos D (2008) Increased plasma homocysteine levels in patients with multiple sclerosis and depression. Ann Gen Psychiatry 7:17

Ungvari Z, Gautam T, Koncz P, Henthorn JC, Pinto JT, Ballabh P, Yan H, Mitschelen M, Farley J, Sonntag WE, Csiszar A (2010) Vasoprotective effects of life span-extending peripubertal GH replacement in Lewis dwarf rats. J Gerontol A Biol Sci Med Sci 65:1145–1156

Vakili H, Jin Y, Cattini PA (2012) Negative regulation of human growth hormone gene expression by insulin is dependent on hypoxia-inducible factor binding in primary non-tumor pituitary cells. J Biol Chem 287(40):33282–33292

Wang Z, Tang L, Zhu Q, Yi F, Zhang F, Li PL, Li N (2011) Hypoxia-inducible factor-1alpha contributes to the profibrotic action of angiotensin II in renal medullary interstitial cells. Kidney Int 79:300–310

Wu CH, Tang SC, Wang PH, Lee H, Ko JL (2012) Nickel-induced epithelial-mesenchymal transition by reactive oxygen species generation and E-cadherin promoter hypermethylation. J Biol Chem 287:25292–25302

Wuhl E, Schaefer F (2002) Effects of growth hormone in patients with chronic renal failure: experience in children and adults. Horm Res 58(Suppl 3):35–38

Yang MH, Wu KJ (2008) TWIST activation by hypoxia inducible factor-1 (HIF-1): implications in metastasis and development. Cell Cycle 7:2090–2096

Yang MH, Wu MZ, Chiou SH, Chen PM, Chang SY, Liu CJ, Teng SC, Wu KJ (2008) Direct regulation of TWIST by HIF-1alpha promotes metastasis. Nat Cell Biol 10:295–305

Yi F, Jin S, Zhang F, Xia M, Bao JX, Hu J, Poklis JL, Li PL (2009a) Formation of lipid raft redox signalling platforms in glomerular endothelial cells: an early event of homocysteine-induced glomerular injury. J Cell Mol Med 13:3303–3314

Yi F, Xia M, Li N, Zhang C, Tang L, Li PL (2009b) Contribution of guanine nucleotide exchange factor Vav2 to hyperhomocysteinemic glomerulosclerosis in rats. Hypertension 53:90–96

Zhang C, Hu JJ, Xia M, Boini KM, Brimson C, Li PL (2010a) Redox signaling via lipid raft clustering in homocysteine-induced injury of podocytes. Biochim Biophys Acta 1803:482–491

Zhang C, Hu JJ, Xia M, Boini KM, Brimson CA, Laperle LA, Li PL (2010b) Protection of podocytes from hyperhomocysteinemia-induced injury by deletion of the gp91(phox) gene. Free Radic Biol Med 48(8):1109–1117

Zhang C, Hu JJ, Xia M, Boini KM, Brimson CA, Laperle LA, Li PL (2010c) Protection of podocytes from hyperhomocysteinemia-induced injury by deletion of the gp91phox gene. Free Radic Biol Med 48:1109–1117

Zhang C, Xia M, Boini KM, Li CX, Abais JM, Li XX, Laperle LA, Li PL (2011) Epithelial-to-mesenchymal transition in podocytes mediated by activation of NADPH oxidase in hyperhomocysteinemia. Pflugers Arch 462:455–467

Zhang T, Qu H, Li X, Zhao B, Zhou J, Li Q, Sun M (2010d) Transmembrane delivery and biological effect of human growth hormone via a phage displayed peptide in vivo and in vitro. J Pharm Sci 99:4880–4891

Zhu Q, Wang Z, Xia M, Li PL, Van Tassell BW, Abbate A, Dhaduk R, Li N (2011) Silencing of hypoxia-inducible factor-1alpha gene attenuated angiotensin II-induced renal injury in Sprague–Dawley rats. Hypertension 58:657–664